Cover Page

Symposium on the Technologies and Metrology of Checkpoint Screening Equipment

05 to 06 April 2017

Toronto, ON

Natural Motion Emulation for Walk-through Metal Detector Testing

Donald R. Larson, Entegra Corporation, Aurora, CO 80016, USA

Nicholas G. Paulter, Jr., National Institute of Standards and Technology, Gaithersburg, MD 20899, USA

Nikolaus F. Troje, Queen's University, Kingston, ON, ON K7L 3N6, Canada

---

The effect of motion through the portal of a walk-through metal detector (WTMD) has often been considered to contribute to the uncertainty in detecting threat objects being carried through the WTMD. However, typical metrological testing uses a robotic system, or similar, to push a test object through the portal with a trajectory that is a straight line and has a constant velocity. This testing, although reproducible and accurate, does not present other than linear trajectories. On the other hand, testing using clean testers, that is, people not carrying any metal objects other than the test object, is not reproducible or accurate because of the great variation between transits through the portal from any one clean tester. We report using a robotic system to accurately study the effect of non-straight-line trajectories of different velocities for the test object passing through the portal of the WTMD.

INTRODUCTION: Walk-through metal detectors (WTMDs) are the mainstay of almost all security checkpoints systems throughout the world. WTMDs can be reliable and their detection results very repeatable and reproducible. WTMDs work by generating an alternating magnetic field that interacts with electrically conductive and/or magnetically permeable objects that are passing through the portal of the WTMD and then sensing the effect of that interaction. WTMDs typically are permanently mounted in a choke point for human pedestrian flow or access but some are designed to be portable. The width of the opening of the portal of the WTMD may vary depending on the security application. The expectations are that the person walking through the portal nominally walks through the center of the portal to avoid bumping the sidewalls of the portal as this will cause the WTMD to alarm until the mechanical vibrations of the sidewalls cease.

The detection performance of WTMDs is tested by passing a metal test object through the portal of the WTMD and noting an alarm indication. Currently this testing is described in the National Institute of Justice standard, NIJ 0601.02, Walk-Through Metal Detectors for Use in Concealed Weapon and Contraband Detection [1]. This transit of the test object may be achieved using a robotic system or a clean tester, which is a person devoid of any metal objects. The use of a robotic system provides results that are much more reproducible and repeatable compared to testing using a clean tester. However, unless the robot is programmed to provide other than straight-line trajectories, natural human motion will not be emulated and the effects of this natural motion on the WTMD detection performance is not tested. A clean tester on the other hand, does present to the WTMD a test object moving with the natural motion of a person. However, this measurement is not reproducible nor repeatable because of the variability in the motion of a person moving through the WTMD portal and, thus, not suitable for accurate assessment of WTMD detection performance, tracking of performance history, or model comparisons.

Table 1. Magnitude of motion (mm) body part, population mean ± standard deviation.

Body part	Anterior-posterior	Lateral	Vertical
center of the head	16.9 ± 7.8	38.5 ± 17.8	47.0 ± 11.9
center of the clavicle	24.7 ± 7.4	30.5 ± 9.5	46.9 ± 11.4
left shoulder	36.8 ± 12.9	32.7 ± 10.5	51.5 ± 14.2
left elbow	181.0 ± 49.2	66.7 ± 20.7	46.9 ± 13.7
left wrist	402.5± 95.1	62.4 ± 34.8	119.2 ± 44.0
right shoulder	37.8 ± 11.7	32.1 ± 10.5	51.2 ± 13.4
right elbow	163.1 ± 51.4	60.9 ± 19.1	47.7 ± 13.54
right wrist	365.3 ± 110.5	52.1 ± 29.0	106.1 ± 38.2
center of pelvis	34.1 ± 7.7	27.9 ± 8.4	46.9 ± 11.5
left hip joint	43.1 ± 11.4	29.7 ± 7.6	48.7 ± 11.1
left knee	331.2 ±36.4	37.7 ± 16.0	85.6 ± 14.7
left ankle	685.5 ± 64.9	38.3 ± 12.8	157.1 ± 18.4
right hip joint	40.6 ± 9.1	29.8 ± 7.4	49.6 ± 11.3
right knee	329.0 ± 34.9	37.0 ± 16.0	83.7 ± 14.9
right ankle	683.5 ± 63.8	38.5 ± 13.7	157.9 ± 18.0

The type of motion that has to be emulated for a test object is important. This type of motion is dependent on where on the body the test object is to be located, for example, the head, hand, or foot. Furthermore, the motion will have a nominal displacement vertically, laterally (side-to-side), and anterior-posterior (front to back) during its transit through the portal. Table 1 provides nominal values for these motions as well as the standard deviation for a sample population, which represents observations of over 440 persons of both genders and ages ranging from 18 years to 60 years [2].

New motion control software was written to enable the robot used to emulate natural human motion. Since natural human motion includes motion in all three dimensions, an array of motion increments was calculated that included the anterior/posterior, lateral, and vertical motions. Each was modeled as cycloids or a lemniscate with appropriate coefficients and phase relationships. For example, with each step, the head moves up/down and left/right. These motions are in phase, starting and ending with the same foot being planted on the ground. The function used to describe motion such as sway and arm swing is the cycloid. It is given by the Cartesian equation:

$$x = a * cos^{-1}(1 - y/a) - \sqrt{2ay - y^2}$$

It may also be described using the parametric form:

$$x = a \times \theta - b \times sin\theta$$

$$y = a - b \times cos\theta$$

A cycloid has three primary variations, normal or common (a=b), curtate (a>b), and prolate (a<b), these shapes are obtained by changing the ratio of the constants “a” and “b” as indicated

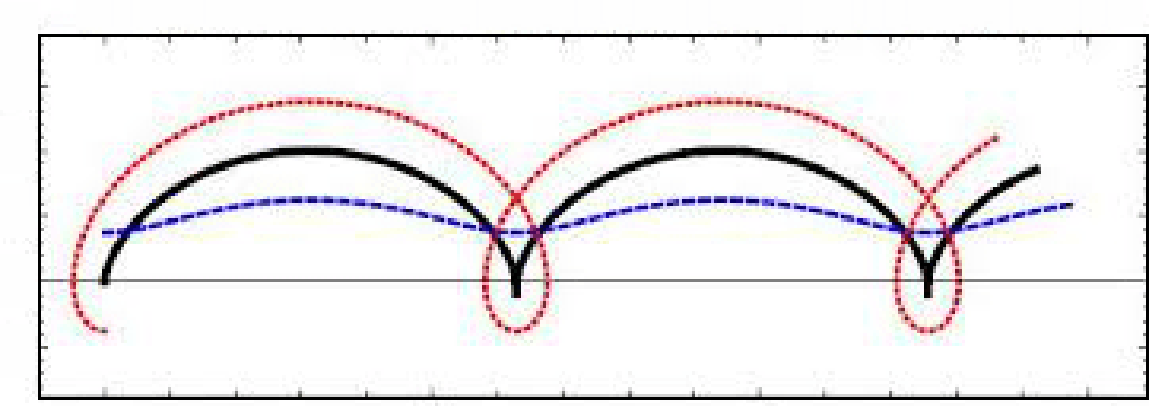

figure 1.

The motion of the foot or heel is more closely emulated using the Lemniscate of Bernoulli; the equation in Cartesian coordinates is given by:

$$[(x - c)^2 + y^2][(x + c)^2 + y^2] = c^4$$

Figure 1. Normal or common (black), curtate (blue), and prolate (red) cycloids.

It is more simply described using the polar form:

$$r^2 = a^2 cos(2\theta)$$

where “a” and “c” are constants. Only the upper quadrant is used (figure 2).

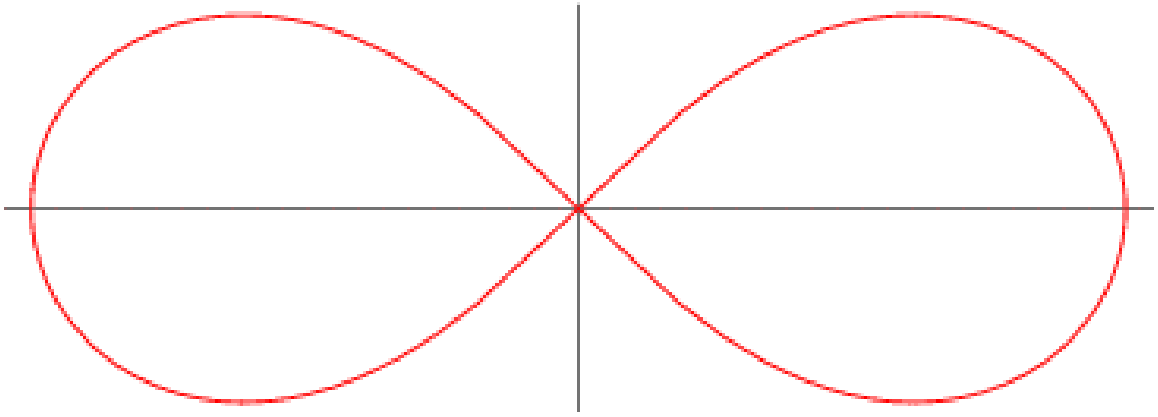

Figure 2. Lemniscate of Bernoulli

The robotic system also recorded the audible alarm indications when a test object was passed through the portal. The robotic system was used to pass two different diameter aluminum spherical test objects. Figures 3 and 4 show the detection map for these two spheres, passing through the WTMD portal along a straight-line trajectory at a velocity of 1 m/s. The trajectory was perpendicular to the plane defined by the WTMD portal, perpendicular to vertical, and parallel to the ground. The aluminum metal spheres were fabricated with UNS A96061 aluminum. Although not the topic of this paper, it is essential that the electrical conductivity and the magnetic permeability of test object be accurately known as this will affect their detectability [3,4]. The nominal diameters of the metal spheres are 35 mm and 24 mm. The spatial increments for the detection alarm maps shown in figures 3 and 4 were nominally 5 cm in both the horizontal and vertical directions.

The detection alarm map shown in Figure 3 is the result of two passes of the test object through the WTMD portal using rectilinear motion. The black indicates zones of high detectability and the white indicates zones of no detectability. Both transits of the 35 mm diameter sphere caused an alarm and further repeated testing was not felt necessary. The 24 mm diameter sphere was detected only at the bottom part of the WTMD portal, as shown in Figure 4. In this case, four transits were used to get a modest understanding of the sphere detectability along the zone between detectable and not detectable. For the four transits and for the 5-cm-spatial increments, the transition between the detectable zone and undetectable zone is abrupt, typically no gray scale.

The aluminum spheres were then pushed through the portal using a cycloid trajectory that is more typical of what is expected if the sphere was attached to or held by the human body. In addition to these trajectories, arbitrary and unrealistic trajectories (such as spirals, zig-zags, etc.) were also tried. All trajectories had a velocity of nominally 1 m/s. The detectability of the 35 mm sphere was not affected by the trajectory through the WTMD portal. Similarly, the

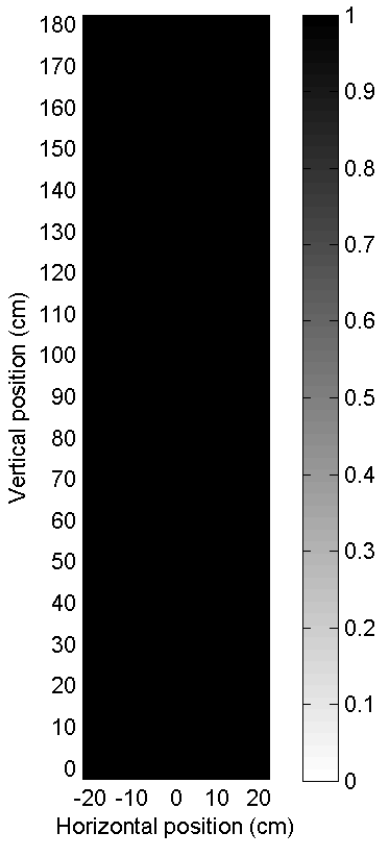

Figure 3. Detection alarm map for 35 mm diameter aluminum sphere.

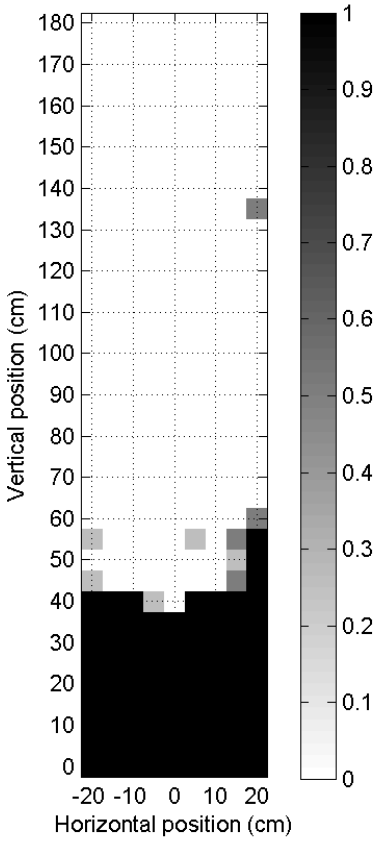

Figure 4. Detection alarm map for 24 mm diameter aluminum sphere.

detectability of the 24 mm sphere was not affected by its trajectory through the WTMD portal. Interestingly, the non-detectability of the 24 mm diameter did not change. The detectability did not improve over the nondetectable zone because the sphere diameter is relatively small and did not interact with adjacent detection zones for the cycloid trajectory used. A WTMD typically comprises several coils for generating magnetic fields, and each of these coils provides a unique detection zone. These zones may overlap.

A knife exemplar, made of aluminum, was also used to assess the effect of trajectory and orientation on the detectability of the exemplar by the WTMD. The knife exemplar is nominally 76 mm long by 19 mm wide by 1.6 mm thick and is fabricated of UNS A95052 aluminum. The general detection zones are similar to what is shown in Figure 4 for all three possible nonequivalent and orthogonal orientations of the knife exemplar. However, depending on the orientation and trajectory of the exemplar, the exemplar could be detected for a cycloid trajectory where it was not detected for a straight-line trajectory. The converse was also true, that the exemplar, although detectable for a straight-line trajectory, could become non-detectable for a cycloid trajectory.

RESULTS/DISCUSSION

The type of trajectory used to test the detectability of spherical test objects was not important, that is, the trajectory did not change the detectability of the sphere for the given spatial increments used. Smaller spatial increments may provide more detail in the transition between the detectability zone and the nondetectability zone. It is not unexpected that the sphere trajectory did not affect its detectability as the magnetic fields within a WTMD are complex and have a fairly uniform strength. Furthermore, the spheres were relatively small, 35 mm diameter and 24 mm diameter, thus not likely to excite more than one detection zone at a time.

The knife exemplar, a thin rectangular prism made of aluminum, exhibited both orientation and trajectory effects on its detectability. The detectability, as evidenced by the generation of an audible alarm by the WTMD, could be increased or reduced depending on both its orientation and trajectory. The increase in detectability is not unexpected for given trajectories because these trajectories could cause the knife exemplar to excite more than one detection zone. However, the decrease in detectability for certain trajectories was not expected, and this is being investigated further.

CONCLUSIONS

The effect of motion through the portal of a walk-through metal detector (WTMD) on the detectability of test objects has been examined. Comparison of the detectability of the test objects with either straight-line or nonstraight-line trajectories using both a robotic system and a manual system was performed for spherical test objects, both measurement systems provide nominally the same result, which is the detectability of the sphere is not affected by its trajectory through the portal. However, this is not the case for nonspherical test objects. The trajectory of the test object, consequently, may contribute to the uncertainty in detecting threat objects being carried through the WTMD. Further investigation is necessary to determine if the effect of test object trajectory on WTMD detection performance should be considered in WTMD performance standards and testing protocols.

REFERENCES

1. National Institute of Justice (2003), Walk-Through Metal Detectors for Use in Concealed Weapon and Contraband Detection. NIJ Standard 0601.02. Available at https://www.ncjrs.gov/pdffiles1/nij/193510.pdf, accessed 06 January 2017.

2. www.biomotionlab.ca, Troje NF, Queen's University, Kingston, Ontario, Canada

3. Janezic MD, Kaiser RF, Baker-Jarvis J, and Free G, (2004) DC Conductivity Measurements of Metals (U.S. Department of Commerce, Washington, D.C.), NIST Technical Note 1531. http://dx.doi.org/10.6028/NIST.TN.1531

4. Janezic MD, Baker-Jarvis J, (2004) Relative Permeability Measurements for Metal Detector Research, (U.S. Department of Commerce, Washington, D.C.), NIST Technical Note 1532. http://dx.doi.org/10.6028/NIST.TN.1532